Volume 1 | Number 1 | Jan 2013 | Pages 1–100

ChemComm

Chemical Communications
www.rsc.org/chemcomm

ROYAL SOCIETY OF CHEMISTRY

ROYAL SOCIETY OF CHEMISTRY

www.rsc.org/chemcomm

Journal Name

COMMUNICATION

A luminescent Dye@MOF as dual-emitting platform for sensing explosives

Xiao-Li Hu, Chao Qin,* Xin-Long Wang, Kui-Zhan Shao and Zhong-Min Su*

An anionic metal–organic framework (MOF) with 1D nanotube channels has been constructed. The charge and size dependent ion-exchange of cationic dyes were investigated. Rho@1 could be used as a dual-emitting fluorescent sensor for the sensing explosives by self-referencing energy transfer behaviors.

Coordination polymers or metal–organic frameworks (MOFs) have developed into a blue-chip research field due to the possibility to obtain a large variety of aesthetically interesting structures [1-2] that could also be of great interest for applications in many fields such as gas storage, luminescence, catalysis, sensing, ion exchange, drug delivery, etc.[3-4] Some of these properties, for example, gas sorption and drug delivery, mainly depend on the pore characteristics of MOFs, including pore size and shape, while others, such as luminescence and sensing, depend on their composition of MOFs, which could be directly applied for chemical sensors.[5] Thus, postsynthetic modification of functional MOFs in response to guest–host interactions is a significant and challenging task. Anionic MOFs have been widely explored for their ion-exchange-based applications which are regarded as postsynthetic methods for obtaining functional MOFs,[6] for example, loading Tb^{3+} and Eu^{3+} to establish the self-calibrated robust temperature and luminescent sensors.[6a,6b]

MOFs in principle can serve as an excellent candidate for chemical sensors to detect trace amounts of nitroaromatic compounds, because the detectable changes in the fluorescence response could be easily achieved by a photo induced electron-transfer mechanism (from π-electron-rich MOFs to π-electron-deficient nitroaromatic compounds).[7] Although such porous MOF approach is promising to act as luminescent sensor, this methodology is limited to single-emission intensity, because the single-emission intensity is variable depending on many uncontrollable factors.[8] Up to now, we only can make use of dual luminescent intensities from different lanthanide ions to establish the luminescent sensors. If luminescent guest species of wider emission wavelengths can be encapsulated into the porous MOFs to form luminescent guest@MOF composites,[9] to make use of the dual-emitting intensity of MOF and luminescent guest species, we can expand the emission ranges to explore novel solid state luminescent sensor. Furthermore, by the inclusion of different luminescent guest theoretically through the spectral overlap between the absorption of luminescent guest and the fluorescence emission of MOFs, the luminescent guest@MOF composite is very appealing to target novel luminescent sensor based on MOF-to-dye energy transfer. [9e]

Herein, we report a new MOF with 1D channels, namely $[(CH_3)_2NH_2]^+[Zn_4(\mu_4\text{-O})(NTB)_2(NO_2\text{-bdc})_{0.5}]\cdot3DMA$ (1) (NTB = 4,4′,4″-nitrilotrisbenzoic acid, NO_2-bdc = 2-nitro-4-benzenedicarboxylicacid), based on triangular carboxylates NTB ligand and $Zn_4(\mu_4$-O) clusters. The anionic MOF can be used to separate large molecules based on ionic selectivity rather than the size-exclusion effect. The charge and size dependent ion-exchange of cationic dyes were investigated. Furthermore, we incorporated organic Rhodamine B dye into 1 to form the Rho@1 composite, which was explored as dual-emitting luminescent platform for sensing explosives.

Compound 1 was obtained by reaction of NTB, NO_2-bdc and $Zn(NO_3)_2\cdot6H_2O$ in DMA solution and its formula elucidated by elemental analysis, single-crystal X-ray diffraction, thermogravimetric analysis (TGA), and charge-balance considerations. The protonated $[(CH_3)_2NH_2]^+$ ions in 1 originate from decarbonylation of dimethylamine. Single crystal X-ray diffraction studies reveal that 1 crystallizes in the monoclinic space group $P2_1/c$. In the asymmetric unit, there are four Zn ions, two NTB ligands and half a NO_2-bdc ligand. Other disordered cations and guest molecules are not crystallographically well-defined. As illustrated in Fig. S1, Zn1, Zn2 and Zn3 are coordinated by three oxygen atoms from three carboxylate NTB and one μ_4-O atom (Zn1–O, 1.920 (2)–1.948 (3) Å; Zn2–O, 1.934 (2)–1.990 (2) Å; Zn3–O, 1.923 (2)–1.978 (2) Å). Different to Zn1-Zn3, Zn4 is linked by three oxygen atoms from three NTB ligands with bridging mode, one oxygen atom from NO_2-bdc ligand and one μ_4-O atom (Zn4–O, 2.000 (2)–2.430(3) Å). The

Institute of Functional Material Chemistry, Key Laboratory of Polyoxometalate Science of Ministry of Education, Northeast Normal University, Changchun, 130024 Jilin, People's Republic of China. E-mail: qinc703@nenu.edu.cn; zmsu@nenu.edu.cn Fax: +86 431-85684009; Tel: +86 431-85099108
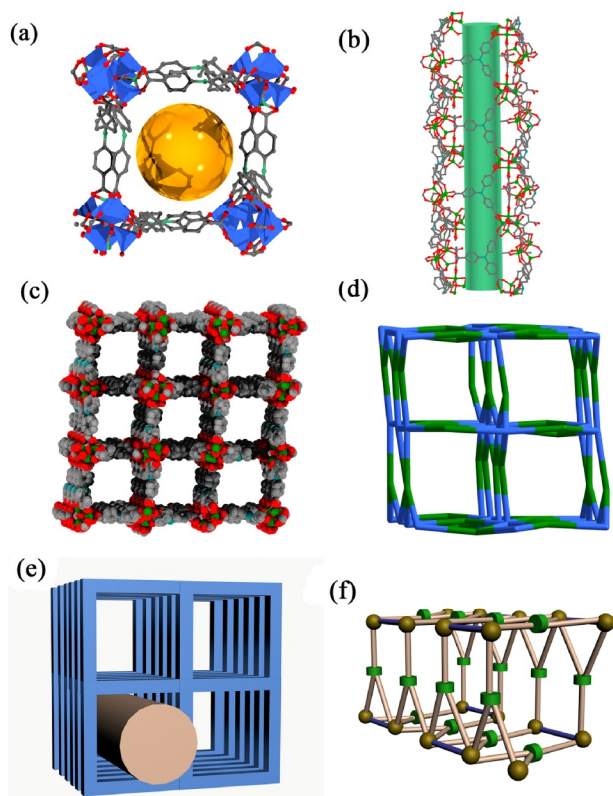
COMMUNICATION

Fig. 1 (a) Polyhedral presentation of 1D channel of 1. (b) Ball-and-stick representation of 1D channel along [101] direction. (c) The representation of 3D packing framework. (d) Schematic representation of the topology of 1. e) and f) 3D presentation of 1D channel running view along [111] direction.

framework of 1 is composed of tetranuclear secondary building unit $[Zn_4O(CO_2)_6]$, which is bridged by the NO_2-bdc ligand to form a one-dimensional chains in a "A-A A" form (A = $[Zn_4O(CO_2)_6]$ SBU, - = NO_2-bdc ligand) (Fig. S2). The distance of adjacent A is 14.97 and 13.78 Å, respectively. The one-dimensional structure is connected by NTB through *in-plane* and *out-of-plane* connectivity to give rise to a 3D structure with one-dimensional channels (Fig. 1).

The square aperture diameter for the one-dimensional channel is 15.0×15.0 Å^2 along the [111] direction. View the side of [101] direction, there is hexagonal pores of approximately 13.9×12.7 Å^2 (Fig. S3). The solvent accessible volumes of 73.2 % (9363.8 Å^3) per unit cell (12784.7 Å^3), is calculated by PLATON.[10] Topological analysis shows that $Zn_4(\mu_4$-O) cluster can be defined as 7-connected nodes, and NTB ligand defined as 3-connected nodes, the architecture of 1 that can be simplified as 3,3,7-connected network with the point symbol of $\{3.5.6\}\{3^2.4^2.5^3.6^{10}.7^3.8\}\{4.5.6\}$.[11]

Overall, the frameworks is anionic with $[(CH_3)_2NH_2]^+$ cations and DMA molecules residing in the nanoscale channels. In order to confirm the phase purity of 1, we measured the powder X-ay diffraction at room temperature (Fig. S4). The experimental X-ray diffraction patterns compared to the corresponding simulated patterns calculated based on single crystal diffraction data, which indicates that all the samples were in a pure phase. The TGA curve of 1 shows that $[(CH_3)_2NH_2]^+$ ions and guest molecules are lost in the temperature range 25–358 ℃ (obsd 20.8 %, calcd 21.4 %) (Fig. S5).

The removal of dyes from effluents before discharge into natural bodies is extremely important from an environmental point of view.

To investigate whether compound 1 has the ability to separate dye molecules, we used them to capture dyes from DMA solutions. Dye molecules with different backbones, sizes and molecular weight and different positive and negative charges were used to perform the ion exchange experiment on 1, respectively (Fig. S6 and Table S2).

Typically, when 30 mg of 1 were soaked in 3 mL DMA solutions of different kinds of dyes, some dye molecules could be efficiently adsorbed over a period of time and the crystals gradually became colored, while others could not be incorporated (Fig. 2). The capability of 1 to adsorb dyes from DMA solution was evaluated through UV/Vis spectroscopy. Spectroscopic investigations of the supernatant showed that 1 can effectively incorporate cationic dyes into their networks, whereas anionic and neutral dyes were left in the supernatants. The selectivity of 1 for dyes could be attributed to the anionic framework, in which the $[(CH_3)_2NH_2]^+$ cations can be exchanged with cationic dyes.

The size of dye is another contributing factor for the ion-exchange process. Three kinds of cationic organic dyes with different sizes but the same charge (Z = +1) were chosen to investigate their ion-exchange processes with 1. The ion-exchange of Methyl Violet (MV) was incomplete after 6 h but the ion-exchange of smaller size Basic Red 2 (BR) and Rhodamine B (RB) were complete in 1 h, although in same concentration (2×10^{-5} mol L^{-1}) (Fig. 3a). The experimental results revealed that the ion-exchange rates for these three dyes were different and related to their dimensions and molecular weights. Generally speaking, when the size of the cationic dye is increased, the ion-exchange process becomes slower. The ion-exchange rates for these three dyes were in the order of BR > RB > MV. The results demonstrated that the size of the anionic guest also plays vital role during ion-exchange process.

To confirm that selective absorption is due to ionic interaction of dye with the anionic framework, dye releasing experiment was performed in pure DMA and a saturated solution of NaCl in DMA
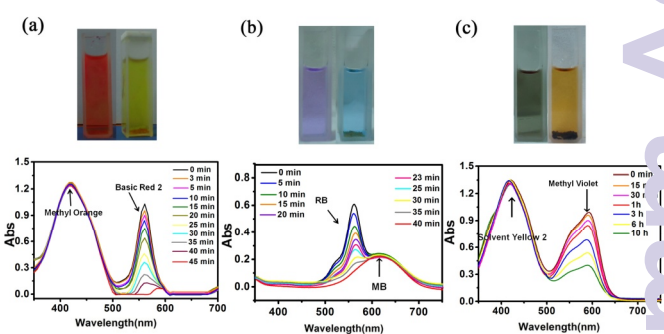

Fig. 2 Photographs and UV/Vis spectra of DMA solutions of dyes with 1: a) Basic Red 2 and Methyl Orange. b) Methylene Blue (MB) and Rhodamine B (RB). c) Methyl Violet and Solvent Yellow 2.

measured by UV/Vis spectroscopy.[12] This showed that, under the triggering of NaCl, the dye molecules in dye@1 and can be gradually released while in DMA without NaCl the dye molecules are hardly released. After 12 h, the release of Basic Red 2 and Rhodamine B dyes was almost complete and the crystalline powder turned back to yellow again (Fig. 3b). Hence, we can safely conclude that selective absorption is due to ionic interaction of dyes with the anionic framework. We had performed such reversible ion exchange process for at least 5 continuous cycles, the powder X-ray
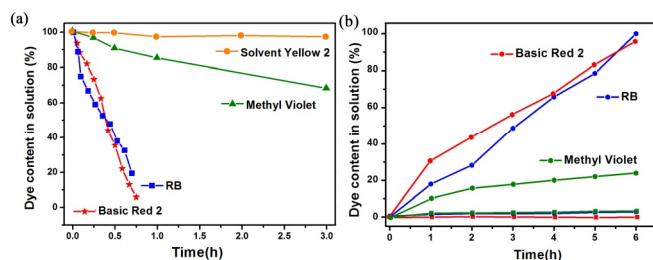
Fig. 3 (a) Temporal evolution of differently sized dyes (+1 charged) content in solution during the ion exchange process. (b) Temporal evolution of dye release in pure DMA (square) and NaCl/DMA (dot).

diffraction of 1 after 5 cycles of exchange-release displayed the same pattern as before, indicating the high stability of the crystalline material (Fig. S4).

The emission spectra of NTB, 1 and Rho@1 were examined at room temperature in the solid state. The free NTB ligand displays an intense and broad band with a maximum at 450 nm in the emission spectrum under 371 nm UV excitation, which is attributed to the π^*-π electron transition. The light emission peak of 1 shifts to 437 nm upon excitation at 369 nm (Fig. S7), which attributed to metal-to-ligand charge transfer (MLCT) and the coordination effects of the NTB to Zn^{2+} ions.[13]

The dye molecules were encapsulated into the pores of 1 by adding crystals in Rhodamine B of DMA solution with different concentrations (2×10^{-5}, 2×10^{-4}, 5×10^{-4}, 1×10^{-3}, 3×10^{-3}, 5×10^{-3} and 8×10^{-3} mol L^{-1}). The precipitated crystals were collected and washed using DMA to remove the residual Rhodamine B dye on the surface of MOF. The content of the Rhodamine B dye in Rho@1 composites were determined to be 0.02 wt%, 0.04 wt%, 0.05 wt%, 0.08 wt%, 0.10 wt%, 0.12 wt%, 0.14 wt% (a-f), respectively, indicating that the desired dye content could be simply obtained by controlling the concentrations of Rhodamine B solution. Moreover, the quantum efficiency of 5.4 % for Rho@1 (f) are higher than that of 1 (2.5 %; excited at 369 nm).

As shown in Fig. 4, the PL spectra of samples exhibit two emission maxima at ~437 and ~589 nm in solid state at room temperature, respectively, when irradiated at 369 nm. The emission at 437 nm is attributed to MLCT in 1 whereas the emission at 589 nm presumably originates from dye Rhodamine B. To determine whether the encapsulation impacts the luminescence properties of the system, we measured the emission spectra of Rhodamine B and a thoroughly ground mixture of Rhodamine B and 1 under the same conditions. Rhodamine B does not display any emission, whereas the mechanically ground mixture only presents the emission band of 1 excited at 369 nm in the solid-state (Fig. S8). It needs to be mentioned that the emission peak profile of Rhodamine B dye in Rho@1 is very similar to that of the Rhodamine B in DMA solution, but significantly different from the behavior of the Rhodamine B in solid state, which displays no emission band (Fig. S9). These results demonstrate that the Rhodamine B dye is uniformly encapsulated in the channels of Rho@1 as free isolated molecules, thus restraining the formation of aggregate or excimer in the solid state dye materials.

Furthermore, Rho@1 has allowed us to systematically tune the emissive light colors by varying the content of the encapsulated Rhodamine B. The PL spectra show that the intensity of the emission at 589 nm increases monotonically as the Rhodamine B amount increases, however, the emission at 437 nm decreases
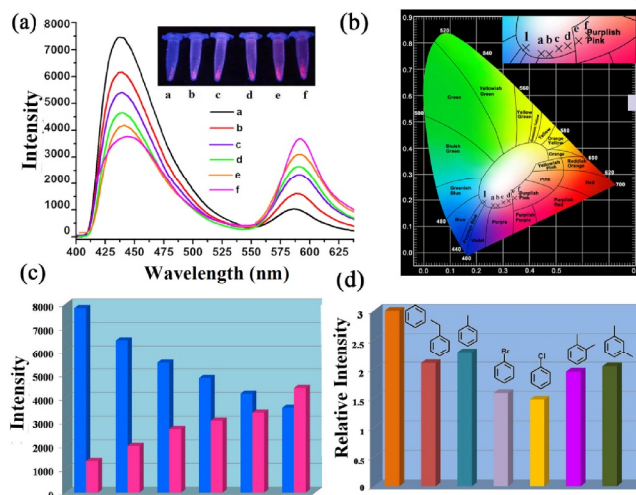

Fig. 4 The emission spectra (a), CIE chromaticitycoordinates (b), emission peak-height ratios of MOF to dye moieties (c), and the solvent-dependent emission peak-height ratios of MOF-to-dye moieties in the luminescence spectra of Rho@1 after adsorption of benzene, toluene, ethylbenzene, Cl-benzene, Br-benzene, o-xylene, m-xylene, p-xylene excited at 369 nm at room temperature (d).

correspondingly. These results demonstrated the MOF-to-dye energy transfer behaviors by effectively adjusting the amounts of included Rhodamine B. The mechanism of MOF-to-dye energy transfer can be attributed to the spectral overlap between the absorption of Rhodamine B and the fluorescence emission of MOFs (Fig. S11).[9c, 9d, 9e] The observed emission colors of Rho@1 match well with the CIE chromaticity diagram, which can be clearly and directly observed with the naked eye (Fig. 4a and Fig. 4b).

The emission spectra of Rho@1 are also temperature-dependent. With the decrease of temperature from 100 to 20 °C, the peak location of Rho@1 at 437 nm and 589 nm remains unchanged, while the intensity of the signal is reduced linearly with decreasing temperature (Fig. S12). The result reveals that Rho@1 will be a potential candidate for applications in temperature-sensing devices.

Considering that the emission peak heights of MOF and dye in Rho@1 are comparable, we explored its sensing capability for various explosives by self-referencing the emission peak heights of MOF and dye moieties in the photoluminescent spectra of Rho@1. Moreover, the luminescent intensity of Rho@1 is highly responsive to different concentrations of the nitrobenzene and TNP (2, 4, 6-trinitrophenol) (Fig. S13). Even small molecules that have very similar structural motifs, such as isomers of o-, m-, and p-xylene, homologues of benzene, toluene, and ethyl-benzene, and halobenzenes, including chloro- and bromobenzene, can read-out by monitoring the relative emission peak-height ratios of MOF to dye moieties, because of their different effects on the energy transfer from MOF to dye moieties (Fig. S14-S16). The stability of the luminescent Rho@1 for sensing has been indicated by recycling experiments (Fig. S17). Remarkably, the relative emission intensity between MOF and dye moieties in the luminescence spectra of Rho@1 is almost constant for 5 cycles in sensing nitrobenzene molecules. These results reveal that Rho@1 could be used as a fluorescent sensor for the detection of explosives with high sensitivity, selectivity, and recyclability.

The results indicate that, in the luminescence spectra of Rho@1, the relative emission intensity of MOF versus dye moieties is

variable to different solvent molecules. Such characteristics can be used to draw an emission-fingerprint map of sensing explosive, based on the photoluminescence of Rho@1. This internal-reference strategy should be able to overcome the drawback of variable emission intensities encountered when probing explosive by a single emissive transition.

Conclusions

In summary, we have synthesized a MOF material containing 1D nanotube channels, and explored the charge and size dependent ion-exchange of cationic dye. These results demonstrated the MOF-to-dye energy transfer behaviors by effectively adjusting the amounts of included Rhodamine B. Remarkably, the luminescent Rho@1 represents a significant step forward in sensing explosives, because of the excellent fingerprint correlation between the explosives and emission peak-height ratio of MOF to dye moieties.

Notes and references

1   (a) H. Furukawa, N. Ko, Y. B. Go, N. Aratani, S. B. Choi, E. Choi, A. ö. Yazaydin, R. Q. Snurr, M. O' Keeffe, J. Kim and O. M. Yaghi, *Science.*, 2010, 329, 424; (b) X. L. Hu, C. Y. Sun, C. Qin, X. L. Wang, H. N. Wang, E. L. Zhou, W. E. Li and Z. M. Su, *Chem Commun.*, 2013, 49, 3564; (c) (d) X. L. Wang, C. Qin, S. X. Wu, K. Z. Shao, Y. Q. Lan, S. Wang, D. X. Zhu, Z. M. Su and E. B. Wang, *Angew. Chem.*, 2009, 121, 5395; *Angew. Chem., Int. Ed.*, 2009, 48, 5291.
2   (a) M. Yoshizawa, J. K. Klosterman, M. Fujita, *Angew. Chem.*, 2009, 121, 3470; *Angew. Chem., Int. Ed.*, 2009, 48, 3418; (b) H. M. He, Y. Song, C. Q. Zhang, F. X. Sun, R. R. Yuan, Z. Bian, L. X. Gao and G. S. Zhu, *Chem. Commun.*, 2015, 51, 9463; (c) J. H. Cavka, S. Jakobsen, U. Olsbye, N. Guillou, C. Lamberti, S. Bordiga and K. P. Lillerud, *J. Am. Chem. Soc.*, 2008, 130, 13850; (d) H, Furukawa, F. Gándara, Y. B. Zhang, J. Jiang, W. L. Queen, M. R. Hudson and O. M. Yaghi, *J. Am. Chem. Soc.*, 2014, 136, 4369.
3   (a) T. M. McDonald, W. R. Lee, J. A. Mason, B. M. Wiers, C. S. Hong, J. R. Long, *J. Am. Chem. Soc.*, 2012, 134, 7056; (b) J. A. Mason, M. Veenstra and J. R. Long, *Chem. Sci.*, 2014, 5, 32; (c) I. Hod, W. Bury, D. M. Karlin, P. Deria, C. W. Kung, M. J. Katz, M. So, B. Klahr, D. Jin, Y. W. Chung, T. W. Odom, O. K. Farha and J. T. Hupp, Adv. Mater., 2014, 26, 6295; (c) X. L. Hu, F. H. Liu, H. N. Wang, C. Qin, C. Y. Sun, Z. M. Su and F. C. Liu., *J. Mater. Chem. A.*, 2014, 2, 14827; (d) P. Q. Liao, D. D. Zhou, A. X. Zhu, L. Jiang, R. B. Lin, J. P. Zhang and X. M. Chen, *J. Am. Chem. Soc.*, 2012, 134, 17380.
4   (a) H. X. Zhong, J. Wang, Y. W Zhang, W. L. Xu, W. Xing, D. Xu, Y. F. Zhang and X. B. Zhang, *Angew. Chem., Int. Ed.*, 2014, 53, 14235; (b) G. Cheng, G. K. M. So, W. P To, Y. Chen, C. C. Kwok, C. Ma , X. Guan, X. Chang, W. M. Kwok and C. M. Che, *Chem. Sci.*, 2015, 6, 4623; (c) T. Zhang and W. B. Lin, *Chem. Soc. Rev.*, 2014, 43, 5982; (d) X. L. Hu, Q. H. Gong, R. L. Zhong, X. L. Wang, C. Qin, H. Wang, J.Li, K. Z. Shao, and Z. M. Su, *Chem. Eur. J.*, 2015, 21, 7238.
5   (a) Y. Q. Lan, H. L. Jiang, S. L. Li, Q. Xu, *Adv. Mater.*, 2011, 23, 5015; (b) X. L. Hu, F. H. Liu, C. Qin, K. Z. Shao and Z. M. Su, *Dalton Trans.*, 2015, 44,7822; (c) P. F Shi, H. C. Hu, Z. Zhang, G. Xiong and B. Zhao, *Chem. Commun.*, 2015, 51, 3985.
6   (a) S. N. Zhao, X. Z. Song, M. Zhu, X. Meng, L. L. Wu, J. Feng, S. Y. Song and H. J. Zhang, *Chem. Eur. J.*, 2015, 21, 9748; (b) J. An, C. M. Shade, D. A. Chengelis-Czegan, S. Petoud and N. L. Rosi, *J. Am. Chem. Soc.*, 2011, 133, 1220; (c) D. T. Genna, A. G. Wong-Foy, A. J. Matzger and M. S. Sanford, *J. Am. Chem. Soc.*, 2013, 135, 10586; (d) B. Li, Y. Zhang, D. Ma, T. Ma, Z. Shi and S. Ma, *J. Am. Chem. Soc.*, 2014, 136, 1202; (e) C. Y. Sun, X. L. Wang, X. Zhang, C. Qin, P. Li, Z. M. Su, D. X. Zhu, G. G. Shan, K. Z. Shao, H. Wu and J. Li, *Nat. Commun.*, 2013, 4, 2717.
7   (a) X. Z. Song, S.-Y. Song, S.-N. Zhao, Z.-M. Hao, M. Zhu, X. Meng, L.-L. Wu and H.-J. Zhang, *Adv. Funct. Mater.*, 2014, 24, 4034; (b) B. Gole, A. K. Bar and P. S. Mukherjee, *Chem.-Eur. J.*, 2014, 20, 2276; (c) S. S. Nagarkar, B. Joarder, A. K. Chaudhari, S. Mukherjee and S. K. Ghosh, *Angew. Chem., Int. Ed.*, 2013, 52, 2881; (d) X. L. Hu, F. H. Liu, C. Qin, K. Z. Shao and Z. M. Su, *Dalton Trans.*, 2015, 44,7822.
8   (a) Z. C. Hu, B. J. Deibert and J. Li, *Chem. Soc. Rev.*, 2014, 43, 5815; (b) B. Gole, A. K. Bar and P. S. Mukherjee, *Chem. Commun.*, 2011, 47, 12137; (c) D. Tian, Y. Li, R. Y. Chen, Z. Chang, G. Y. Wang, X. H. Bu, *J. Mater. Chem. A.*, 2014, 2, 1465; (d) Y. Salinas, R. Martinez-Manez, M. D. Marcos, F. Sancenon, A. M. Castero, M. Parra and S. Gil, *Chem. Soc. Rev.*, 2012, 41, 1261.
9   (a) Q. L. Zhu, Q. Xu, *Chem. Soc. Rev.*, 2014, 43, 5468; (b) Y. Cui, Y. Yue, G. Qian and B. Chen, *Chem. Rev.*, 2012, 112, 1126; (c) M. J. Dong, M. Zhao, S. Ou, C. Zou and C. D. Wu, *Angew. Chem., Int. Ed.*, 2014, 53, 1575; (d) C. Y. Sun, X. L. Wang, X. Zhang, C. Qin, P. Li, Z. M. Su, D. X. Zhu, G. G. Shan, K. Z. Shao, H. Wu and J. Li, *Nat. Commun.*, 2013, 4, 2717; (e) Y. J. Cui, R. J. Song, J. C. Yu, M. Liu, Z. Q. Wang, C. D. Wu, Y. Yang, Z. Y. Wang, B. L. Chen and G. D. Qian, *Adv. Mater.*, 2015, 27, 1420; (f) Z. Dou, J. Yu, Y. Cui, Y. Yang, Z. Wang, D. Yang and G. Qian, *J. Am. Chem. Soc.*, 2014, 136, 5527.
10 A. L. Spek, PLATON, A multipurpose crystallographic tool, Utrecht. University, The Netherlands, 2003.
11 (a) V. A. Blatov and A. P. Shevchenko, TOPOS-Version 4.0 Professional (Beta Evaluation) , Samara State University, Samara, Russia, 2006; (b) V. A. Blatov, A. P. Shevchenko and V. N. Serezhkin, J. *Appl. Crystallogr.*, 2000, 33, 1193; (c) V. A. Blatov, *Struct. Chem.*, 2012, 23, 955.
12 (a) C. Y. Sun, X. L. Wang, C. Qin, J. L. Jin, Z. M.Su, P. Huang and K. Z. Shao, *Chem. Eur. J.*, 2013, 19, 3639; (b) J. T. Jia, F. X. Sun, T. Borjigin, H. Ren, T. T. Zhang, Z. Bian, L. X. Gao and G. S. Zhu, *Chem. Commun.*, 2012, 48, 6010; (c) C. M. Doherty, D. Gao, B. Marmiroli, H. Amenitsch, F. Lisi, L. Malfatti, K. Okada, M. Takahashi, A. J. Hill, P. Innocenzi and P. Falcaro, *J. Mater. Chem.*, 2012, 22, 16191; (d) Y. C. He, J.Yang, W. Q. Kan, H. M. Zhang, Y. Y. Liu and J. F. Ma, *J. Mater. Chem. A.*, 2015, 3, 1675.
13 (a) Q. Zhang, A. Geng, H. Zhang, F. Hu, Z. H. Lu, D. Sun, X. Wei and C. Ma, *Chem. -Eur. J.*, 2014, 20, 4885; (b) J. R. Lakowicz, *Principles of Fluorescence Spectroscopy*, 3rd ed., Springer, Berlin, 2006.